Electronic and structural properties of micro-and nanometre-sized crystalline copper monoxide ceramics investigated by positron annihilation

2002 J. Phys.: Condens. Matter 14 7981

(http://iopscience.iop.org/0953-8984/14/34/317)

INSTITUTE OF PHYSICS PUBLISHING JOURNAL OF PHYSICS: CONDENSED MATTER

J. Phys.: Condens. Matter **14** (2002) 7981–7990 PII: S0953-8984(02)35939-3

Electronic and structural properties of micro- and nanometre-sized crystalline copper monoxide ceramics investigated by positron annihilation

A P Druzhkov[1,3], B A Gizhevskii[1], V L Arbuzov[1], E A Kozlov[2], K V Shalnov[1], S V Naumov[1] and D A Perminov[1]

[1] Institute of Metal Physics, Ural Branch Russian Academy of Sciences, 18 S Kovalevskaya St, 620219 Ekaterinburg, GSP-170, Russia
[2] All-Russian R&D Institute of Technical Physics, Snezhinsk, Russia

E-mail: druzhkov@imp.uran.ru

Received 17 April 2002
Published 15 August 2002
Online at stacks.iop.org/JPhysCM/14/7981

Abstract

Electronic and structural properties of copper monoxide (CuO) sintered as a common ceramic and nanoceramic are studied by positron annihilation spectroscopy. A CuO nanoceramic with crystallite size ranging from 15 to 90 nm was prepared from a common one by shock-wave loading. It is found that the momentum distribution of valence electrons in CuO is shifted, as compared with metallic copper, towards higher momentum values. This result is related to the effect of the Cu 3d–O 2p hybridization in the Cu–O ionic covalent bond formation. It is found that open volumes, identified mainly as small agglomerates of oxygen vacancies, appear at the nanoceramic crystallite interfaces. The degree of the Cu–O bond covalency decreases locally at the crystallite interfaces because of an oxygen deficit. The nanocrystalline state in CuO is shown to be thermally stable up to 700 K.

1. Introduction

Copper monoxide (CuO) is under active study as the chemical basis of cuprate high-temperature superconductors [1]. It is also of prospective use in photosensitive elements [2] and catalysts [3]. Ceramics with nanometre-sized grains (crystallites) or so-called nanoceramics are most efficient in the catalysis of chemical reactions. Size effects are found to cause changes in the specific features of the chemical bond [4] and magnetic properties [5] and also are significant for the efficiency of CuO-based structures in gas sensors [6].

[3] Author to whom any correspondence should be addressed.

Thus, it is very important to understand the interrelation of the crystallite interface features and electronic properties in nanoceramics since the properties of these interfaces make the difference between the properties of the common and nanosized states. Since nearly all the studies concerned with nano-CuO have been performed using either nanopowders or low-compact sintered samples [4, 7], the examination of a compact nanoceramic presented in this paper is of special interest. Also, the knowledge of the temperature range of the nanocrystalline state stability is of significant interest for practical applications.

This study deals with the electronic and structural properties of a copper monoxide with crystallites of the common micrometre scale and a high-density CuO nanoceramic prepared by the shock-wave loading method [8]. Positron annihilation spectroscopy (PAS) having a dual application was used. Firstly, the angular correlation of the annihilation radiation (ACAR) gives information on electronic properties of the analysed material, specifically the momentum distribution of the valence and core electrons [9]. Secondly, positrons are extremely sensitive to atomic defects like the open volume [10]. In addition to the examination of metals and semiconductors [11, 12], PAS has been used widely in the last decade for analysis of structural and electronic properties of both oxide superconductors [13, 14] and nanocrystalline materials [15, 16]. In compacted nanomaterials with a crystallite size much smaller than the positron diffusion length ($L_+ \sim 100$ nm [17]), positrons are trapped at defects like the open volume (vacancies and their agglomerates) located at crystallite interfaces. In this case parameters of the annihilation radiation provide information on the structure of crystallite interfaces.

The core electrons are tightly bound to nuclei and thus the high-momentum parts of the ACAR spectrum carry information on the type of atom in the region scanned by the positron [18–20]. Therefore the annihilation of trapped positrons with surrounding core electrons reveals chemical information. The study also employs this approach for identifying the local chemical environment of positron annihilation sites.

2. Materials and experimental technique

The copper oxide ceramic was prepared from a high-purity (99.99%) CuO powder with grains 5–15 μm in size. The powder was compacted under static conditions at 200 MPa and then sintered in air at 1173 K for 4 h. The obtained ceramic density accounted for about 80% of the theoretical value.

The nanoceramic was produced from the CuO ceramic by subjecting it to shock-wave loading [8]. A layer of a hexogen-based explosive was set off on the surface of a spherical sealed stainless-steel casing, which housed a sphere of the CuO ceramic. The sealed casing did not break upon explosion and, therefore, the material was not polluted during the compaction process. The microstructure of the nanoceramic prepared by this method was certified using x-ray diffraction and scanning tunnelling microscopic (STM) analyses [21]. Most ($\sim$80%) of the volume of the compacted CuO sphere represented a nanoceramic (n-CuO) with crystallites less than 100 nm in size and the density accounting for over 97% of the theoretical value.

CuO ceramic plates, 10 mm $\times$ 10 mm $\times$ 2 mm in size, polished mechanically and then etched chemically, were used for the PAS measurements. n-CuO plates with the same dimensions were cut out at right angles to the radius of the compacted sphere. The crystallite size in the samples was varying in a wide range from 15 to 90 nm because of a difference in loading conditions along the radius of the compacted sphere [21].

To reveal the temperature range of the n-CuO stability the samples of the latter were stepwise annealed (50–100 K in each step) in air over a temperature range from 300 to 1173 K at an average heating rate of 1 K min^{-1}.

Samples made of well annealed pure copper and monocrystalline silicon were also used in PAS measurements as references.

ACAR (one of the PAS methods) used in the study was realized in a one-dimensional ACAR spectrometer providing a resolution of 1 mrad × 160 mrad [20]. The ACAR spectra represent the dependence of the coincidence count rate on the angle θ. The angle $\theta = p_z/m_0c$, where p_z is the transverse component of the momentum of an electron–positron pair, m_0 is the rest mass of an electron and c is the light velocity. The ACAR data contain information on the momentum distribution of annihilating electrons [9] and it is possible to separate the contributions from the annihilation of positrons with valence electrons (the low-momentum part of the spectrum) and core electrons (the high-momentum part of the spectrum). The lattice crystal field has little effect on strongly bound (core) electrons and therefore the high-momentum part of the ACAR spectrum bears information on the type of atom at a positron annihilation site.

The ACAR spectra of the CuO and n-CuO were approximated by two Gaussians, while those of Cu and Si were approximated by an inverted parabola and a Gaussian. The approximation of the experimental spectra considering the spectrometer resolution function has been described in detail elsewhere [22]. The approximation quality criterion approached unity. The contributions of valence and core electrons to ACAR spectra were determined from ratio curves [19]. The latter were obtained in the following way: approximated ACAR spectra were normalized to a unit area and then the CuO and n-CuO spectra were divided by spectra of reference elements. Cu and Si have been taken as the reference elements, since copper is a part of the compound and silicon has a relatively simple structure of the ionic core.

Variations in the shape of the ACAR spectra were characterized by standard S- and W-parameters [20]. The S- and W-parameters were defined as a ratio of the sum of the coincidence count rate over θ range from 0 to 3.5 and 10 to 15 mrad to the full coincidence count rate respectively. The S- and W-parameters characterize the probability of annihilation of positrons with valence electrons and core electrons respectively. When positrons are trapped at open volume defects, the S-parameter grows and the W-parameter diminishes [10].

3. Results and discussion

3.1. The common CuO ceramics

The parameters of the CuO ACAR spectrum are given in table 1, together with the data obtained for copper and silicon. A large value of the full width at half maximum (FWHM) of the CuO ACAR spectrum as compared to the FWHM in the metal (Cu) and the classical semiconductor (Si) is remarkable. It should be noted that an unusually wide ACAR spectrum is typical for NiO [23] and other transition-metal oxides [24], and also cuprate superconductors, such as $YBa_2Cu_3O_{7-\delta}$ [25] and La_2CuO_4 [14]. One more specific feature of the CuO ACAR spectrum consists in a relatively high value of the W-parameter, which attests to a considerable contribution of the core electrons to the full annihilation rate [20].

The contribution of core and valence electrons to the positron annihilation probability densities in CuO can be more readily illustrated by ratio curves. Figure 1 presents ratio curves of copper and CuO with respect to Si. These ratio curves directly reflect the contribution of core electrons, because the contribution of intrinsic Si core electrons (mainly 2p-states) is small enough (2–3%) [26]. The momentum p_z is given in m_0c units. At the momentum values exceeding $8 \times 10^{-3}\ m_0c$, the copper curve exhibits a wide peak corresponding to the annihilation of positrons with 3d electrons [27]. The ratio curve of CuO also has a peak at those momentum values, but this peak is narrower and less intensive.

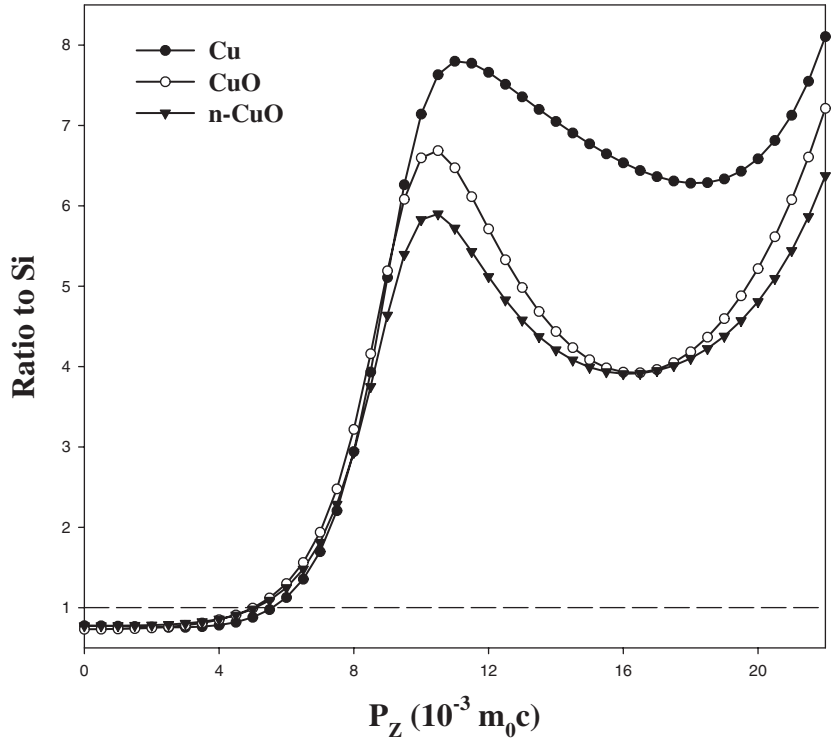

Figure 1. Ratio curves of the ACAR spectra of Cu, CuO and n-CuO with respect to that of Si.

Table 1. Parameters of the ACAR spectra in several materials.

Material	*S*-parameter (arb. units) ±0.0015	*W*-parameter (arb. units) ±0.001	FWHM (mrad) ±0.1
CuO	0.5250	0.067	13.0
Cu	0.5341	0.092	10.6
Si	0.6922	0.012	10.0
n-CuO	0.5550	0.060	11.5
n-CuO ($T_{ann} = 1173$ K)	0.5270	0.068	12.9

Let us discuss the features of the latter curve. The lattice in CuO has a monoclinic symmetry [28]. Each atom has four nearest neighbours of another kind: copper atoms are at the centre of an oxygen rectangle, while oxygen atoms are at the centre of a distorted copper tetrahedron. It is commonly assumed [14, 29] that the delocalized Bloch states of positrons are realized in perfect oxide compounds. We shall assume that this is valid in CuO also. A positron trapping at structural vacancies is highly improbable, because the homogeneity interval of CuO is very narrow and this compound is nearly stoichiometric at room temperature [30]. Positrons are also insensitive to micrometre-scale voids inevitably present in the common ceramics (the density is only 80% of the theoretical value).

So, the observation of a peak in the oxide over the same momentum value range as in the metallic copper suggests that the delocalized positrons annihilate in the CuO with mainly 3d electrons of copper ions. As is known [28], CuO represents an antiferromagnetic

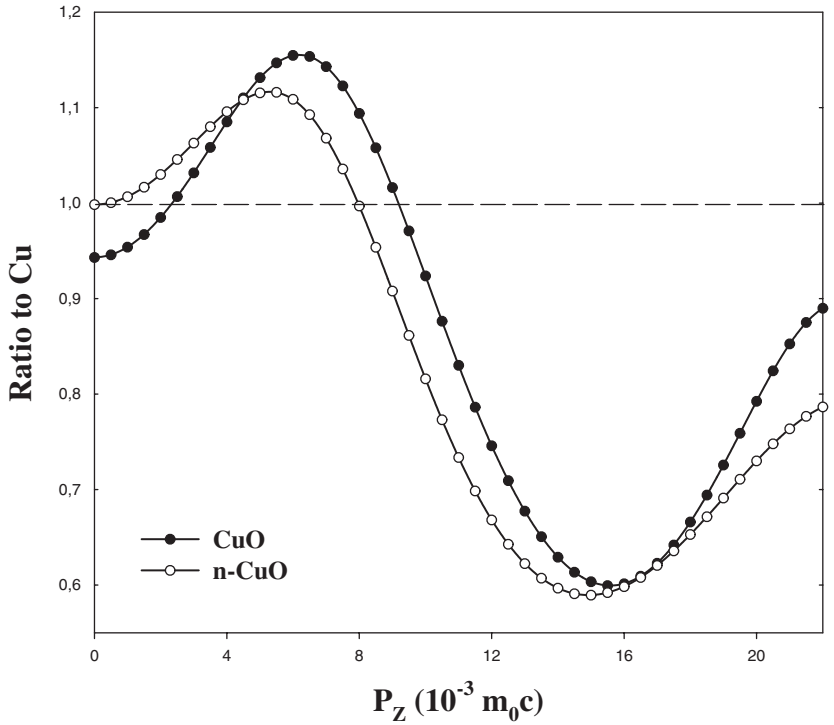

Figure 2. Ratio curves of the ACAR spectra of CuO and n-CuO with respect to that of Cu.

semiconductor with an ionic covalent chemical bond and the covalent component is formed as a result of the Cu 3d–O 2p hybridization. Therefore the occupancy has to decrease due to hybridization and this is confirmed by recent data on the 3d-state occupancy, equal to ≈9.3 electrons [31] instead of 10 in metallic copper. Thus the partial involvement of 3d electrons in the chemical bond might be one of the factors mainly responsible for a peak height decrease in the CuO.

The specific features of the chemical bond should manifest themselves in the low-momentum (valence) part of the ACAR spectrum. In this case, the ratio curve with respect to the metallic copper (figure 2) proved unexpectedly to be most informative. As is seen from the figure, an enhanced momentum density is observed within the low-momentum region (3–9 $\times$ 10^{-3} m_0c) in the CuO. These relatively high momentum density values of valence electrons (the peak of valence electrons) as compared to conduction electrons of the metal might point to an interference of copper 3d and oxygen 2p states. Indeed, the calculations made within the LCAO-MO (molecular orbital as a linear combination of atomic orbitals) scheme in Fe_3O_4 [29] showed that even a small degree of covalency fully modifies the momentum distribution. In particular, mixing of Fe 3d t_{2g} and O 2p orbitals leads to an increase in the momentum distribution density around (5–8) $\times$ 10^{-3} m_0c. Thus the CuO ratio curve with respect to a pure metal allows us to obtain valuable information on electron density variations for valent states.

Lower momentum density values observed in the high-momentum part of the CuO curve (figure 2) obviously are due to the above-mentioned decrease in the contribution of the localized 3d states to the positron annihilation probability as compared to metallic copper.

3.2. The nanoceramics

The annihilation of positrons in the nanocrystalline ceramics is characterized by the narrowing of the ACAR spectrum. The FWHM decreases up to 11.5 mrad with an initial value equal to 13 mrad. The *S*-parameter grows, while the *W*-parameter drops (see table 1). An examination of nanocrystalline materials by PAS shows [15] that with the crystallite size much smaller than the positron diffusion length, positrons are mainly trapped at open volume defects (vacancies, vacancy agglomerates and nanovoids) at crystallite interfaces. The trapped positron annihilation parameters are very sensitive to the open volume of the defects and can vary significantly depending on the technology of nanomaterial production [15, 16]. According to [15, 16] the positronium quasi-atoms (which exist in two states, *para*- and *ortho*-ones) can be formed in nanovoids with size about the size of crystallites. A decay of the *ortho*-state can be detected by positron lifetime measurements while that of the *para*-one can be seen by means of ACAR. A decay of *para*-positronium state causes a considerable narrowing of the ACAR spectrum: FWHM ranges from 3 to 8 mrad depending on the size of the nanovoids [32]. As shown above, the spectrum of our n-CuO narrows little and therefore it may be inferred that the n-CuO samples under study are free of nanovoids. This conclusion agrees well with a high compactness (up to 97% of theoretical value) of our nanoceramics. Single micrometre-scale voids (cracks), which may be present in large n-CuO samples, have a negligible effect on the ACAR spectra because of their small concentration.

Since data concerned with positron states in CuO are not available now it is reasonable to refer to the data in cuprate superconductors, in which as in CuO the positron density is concentrated near Cu–O bonds [13, 14]. The *S*-parameter increment in n-CuO (as compared with common CuO) is close to the value of the *S*-parameter increase in $YBa_2Cu_3O_{7-\delta}$ with the oxygen deficit parameter δ varying from zero to unity [33]. According to the calculation [13], the positron affinity is enhanced with decreasing oxygen content, i.e. positrons have a strong tendency to localize in the oxygen-deficient zones. On the other hand, single oxygen vacancies are found to be only weak traps for positrons. Considering the aforementioned facts, the authors of [33] concluded that the increase in the *S*-parameter (and the lifetime) in $YBa_2Cu_3O_{7-\delta}$ in high-temperature equilibrium experiments was due to a loss of oxygen from Cu(1)–O(1) planes and trapping of positrons at anion vacancy complexes. Therefore is reasonable to discuss the probable interrelation of positron annihilation parameters in n-CuO with the local oxygen deficiency.

As is seen in figure 1 the peak position in n-CuO fully coincides with that in CuO, but the peak height is smaller. This is possible if positrons in the nanoceramics also annihilate with localized 3d electrons of copper ions, but the probability of this process is smaller. Such a situation is typical for positrons being trapped at open volume [34]. The positron wavefunction becomes localized within the open volumes and its overlapping with wavefunctions of the nearest ion core electrons drops leading to a subsequent drop in both the annihilation rate with the core electrons as well as the amplitude of momentum distribution. As follows from the n-CuO ratio curve (figure 1), copper ions are nearest to positron annihilation sites. Therefore it could be concluded that the vacant sites namely in the anion sublattice act as positron traps, because the distance between copper and oxygen ions is the shortest (1.95 Å) [28] in a monoclinic cell of CuO. If positrons were trapped at cation vacancies, the peak in the ratio curve (figure 1) would not have been observed, since the probability of the positron annihilation with 1s electrons of oxygen is small owing to a strong Coulomb repulsion of the nucleus. Nevertheless the effects of positron trapping at cation vacancies cannot be neglected completely. For example, the local non-stoichiometry at the crystallite interfaces can lead to the appearance of Cu atoms in the nearest neighbour shell of the Cu vacancy. Also, the

positron wavefunction may extend to the next nearest Cu vacancy neighbours where Cu atoms dominate. These processes can contribute to the 3d electron momentum distribution but the value of this contribution in our opinion is not essential. Both sufficiently high values of the 3d electron momentum distribution peak height in n-CuO and theoretical and experimental results in cuprate superconductors [13, 33] point to the dominant positron trapping at oxygen deficit zones, therefore giving evidence in favour of such an assumption. Thus the dominant positron traps are presented by open volume as oxygen-vacancy-like defects.

The local zones of non-stoichiometry in the anion sublattice of the nanoceramics also have to affect the other physical properties such as electrical resistivity. An increase in the nanoceramic electrical resistivity is observed and also related to a deviation from stoichiometry [35]. It is thought that the deviation from the stoichiometry due to the oxygen deficit leads to the formation of Cu^+ ions. Since CuO has a p-type conductivity [36], Cu^+ ions represent donors and compensate the initial hole conductivity giving a rise in electrical resistivity correspondingly. Recent studies of n-CuO by x-ray photoelectron spectroscopy and x-ray emission spectroscopy [37] revealed some quantity of the reduced Cu_2O phase in the nanoceramics. These facts also point indirectly to the partial oxygen deficit and formation of anion-vacancy-like defects in n-CuO.

The peak of valence electrons in n-CuO shifts towards lower momentum values as compared to that in CuO (figure 2). This testifies both to trapping of positrons at vacancy-like defects and a partial disturbance of ionic covalent (or the covalent component) Cu–O bonds owing to an oxygen deficit and, hence, a redistribution of the electronic density. An increase in the ionicity of Cu–O bonds with decreasing size of CuO nanoparticles was also observed by x-ray photoelectron spectroscopy [4], giving independent evidence in favour of the above.

If all observed peculiarities of positron annihilation in n-CuO as compared to common CuO are related to the positron trapping at oxygen deficit zones at crystallite interfaces they have to recover during recrystallization. But determination of the mean crystallite size is strongly complicated by a large scattering in crystallite size (15–90 nm) in the whole sample. To reduce this effect and reveal the kinetics of crystallite growth the STM measurements were made approximately at one and the same local point of the n-CuO sample, which was used in the ACAR series. Nevertheless even in this case a wide crystallite size spectrum leads to a large scattering in mean crystallite size data.

As seen in figure 3 correlation between variations in the S-parameter and the crystallite size during the thermal annealing of n-CuO is observed: the S-parameter values in n-CuO are shifted towards the values in common CuO during recrystallization. The crystallite size and S-parameter recovery start to occur at temperatures above 600–650 K. The S-parameter attains values characteristic of coarse-grained CuO at 1100 K. The parameters of the ACAR spectra and ratio curve (figure 4) also recover values typical of common CuO at 1173 K (see table). The above data give direct evidence in favour of the oxygen deficit zone location at crystallite interfaces. Additionally a very important conclusion can be made that despite a wide size distribution of the crystallites (15–90 nm) in the initial n-CuO positrons diffuse with high probability ($L_+ \approx 100$ nm) from the interior of the crystallites into the traps at interfaces without measurable annihilation in the bulk state. Another conclusion which follows from the data is that the n-CuO state is thermally stable up to 700 K. This temperature is high enough for nanostructured materials and allows extension of the range of applications of the CuO nanoceramics prepared by the method of shock-wave loading.

Unfortunately nothing can be said about whether the positron annihilation parameter recovery starts simultaneously with the crystallite size growth or some delay between these two processes occurs. Such information could shed light on the details of the crystallite interface intrinsic structure.

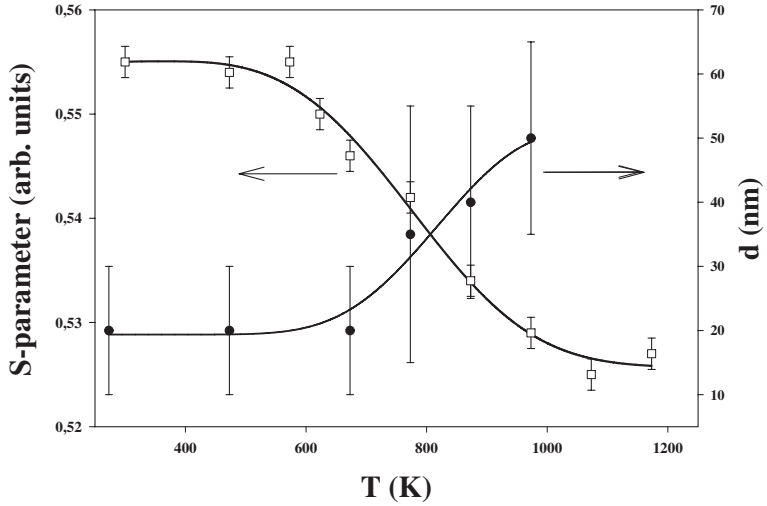

Figure 3. Stepwise annealing of nanocrystalline CuO. *S*-parameter (□) and crystallite size *d* (●).

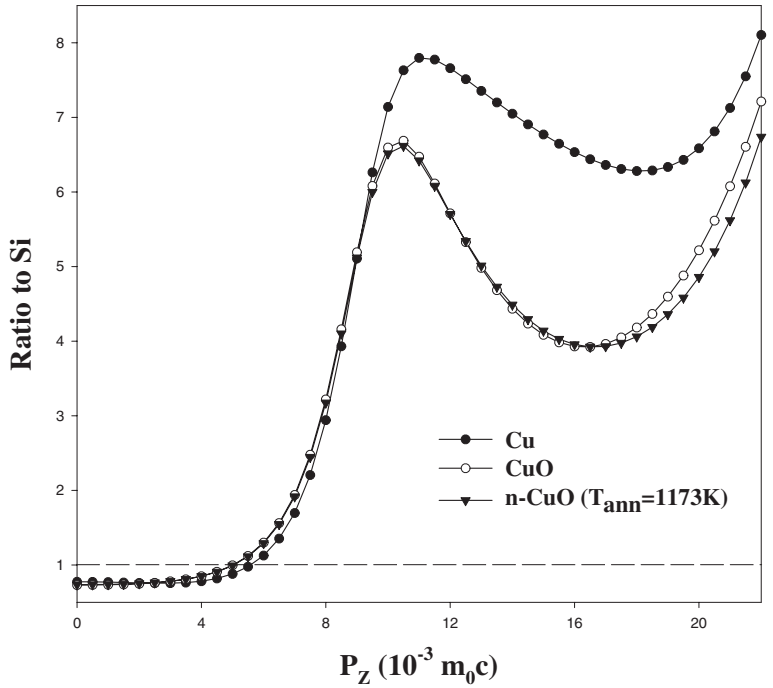

Figure 4. Ratio curves of the ACAR spectra of Cu, CuO and n-CuO after annealing at 1173 K with respect to that of Si.

4. Summary and conclusions

Electronic and structural properties of a copper monoxide prepared by thermal sintering and shock-wave loading methods with micro- and nanometre-sized crystallites respectively were investigated by PAS. The obtained results may be summarized as follows.

(i) The momentum distribution of valence electrons in CuO is shifted, as compared with metallic copper, towards higher momentum values. This shift is attributed to specific features of the ionic covalent Cu–O bond, specifically, the Cu 3d–O 2p hybridization.

(ii) It is found that open volumes, which are identified, mainly, as anion-vacancy-like defects, appear at the crystallite interfaces in the nanoceramics. An oxygen deficit in these open volumes leads to a decrease in the degree of Cu–O bond covalency at the crystallite interfaces.

(iii) Nanovoids were not detected and this testified to a high quality of the nanoceramics obtained by a shock-wave loading method. The nanoceramics prepared by this method were found to be thermally stable up to 700 K.

Acknowledgments

This study was performed with financial support from the Russian Foundation for Basic Research (grant No 01-02-96403). The authors want to thank Dr Alexander Nikolaev for critical reading and editing of the text.

References

[1] Dagotto E 1994 *Rev. Mod. Phys.* **66** 763–840
[2] Sebastion P J 1996 *Mater. Manuf. Process.* **11** 215–24
[3] Ahmad A S, Elshobaky G A, Alnoaini A N and Elshobaky H G 1996 *Mater. Lett.* **26** 107–12
[4] Borgohain K, Singh J B, Rama Rao M V, Shripathi T and Mahamuni S 2000 *Phys. Rev.* B **61** 11 093–6
[5] Arbuzova T I, Naumov S V, Samokhvalov A A, Gizhevsky B A, Arbuzov V L and Shalnov K V 2001 *Fiz. Tverd. Tela* **43** 846–50
[6] Wei Q, Luo W D, Liao B, Liu Y and Wang G 2000 *J. Appl. Phys.* **88** 4818–24
[7] Garcia-Martinez O, Rojas R M, Vila E and Martin de Vidales J L 1993 *Solid State Ion.* **63–65** 442–9
[8] Kozlov E A and Gizhevsky B A 1998 Compacting CuO ceramics using spherical shock isentropic waves *Preprint* Zababakhin All-Russia Research Institute of Technical Physics, Russian Federal Nuclear Centre, Snezhinsk, no 137
[9] Berko S 1983 *Positron Solid State Physics* ed W Brandt and A Dupasquier (Amsterdam: North-Holland)
[10] Siegel R W 1980 *Annu. Rev. Mater. Sci.* **10** 393–425
[11] Eldrup M and Singh B N 1997 *J. Nucl. Mater.* **251** 132–8
[12] Corbel C 1992 *Mater. Sci. Forum* **105–110** 221–8
[13] Jensen K O, Nieninen R M and Puska M J 1989 *J. Phys.: Condens. Matter* **1** 3727–32
[14] Turchi P E A, Wachs A L, Wetzler K H, Kaiser J H, West R N, Jean Y C, Howell R H and Fluss M J 1990 *J. Phys.: Condens. Matter* **2** 1635–58
[15] Schaefer H-E, Wurschum R, Birringer R and Gleiter H 1988 *Phys. Rev.* B **38** 9545–54
[16] Wurschum R 2001 *Mater. Sci. Forum* **363–365** 35–9
[17] Puska M J and Nieminen R M 1994 *Rev. Mod. Phys.* **66** 841–97
[18] Alatalo M, Kauppinen H, Saarinen K, Puska M J, Makinen J, Hautojarvi P and Nieminen R M 1995 *Phys. Rev.* B **51** 4176–85
[19] Asoka-Kumar P, Alatalo M, Ghosh V J, Kruseman A C, Nielsen B and Lynn K G 1996 *Phys. Rev. Lett.* **77** 2097–100
[20] Arbuzov V L, Danilov S E and Druzhkov A P 1997 *Phys. Status Solidi* a **162** 567–73
[21] Gizhevsky B A, Kozlov E A, Ermakov A E, Lukin N V, Naumov S V, Samokhvalov A A, Arbuzov V L, Shalnov K V and Degtyarev M V 2001 *Fiz. Met. Metalloved.* **92** 52–7 (Engl. transl. 2001 *Sov. Phys.–Met. Metallogr.* **92** 153–7)
[22] Rempel A A, Druzhkov A P and Gusev A I 1989 *Fiz. Met. Metalloved.* **68** 271–9 (Engl. transl. 1989 *Sov. Phys.–Met. Metallogr.* **68** 59–68)
[23] Chiba T and Tsuda N 1974 *Appl. Phys.* **5** 37
[24] Akahane T, Hoffmam K R, Chiba T and Berko S 1985 *Solid State Commun.* **54** 823–6
[25] von Stetten E C, Berko S, Li X S, Lee R R, Brynestad J, Singh D, Krakauer H, Pickett W E and Cohen R E 1988 *Phys. Rev. Lett.* **60** 2198–201

[26] Alatalo M, Barbiellini B, Hakala M, Kauppinen H, Korhonen T, Puska M J, Saarinen K, Hautojarvi P and Nieminen R M 1996 *Phys. Rev.* B **54** 2397–409
[27] Ghosh V J, Alatalo M, Asoka-Kumar P, Nielsen B, Lynn K G, Kruseman A C and Mijnarends P E 2000 *Phys. Rev.* B **61** 10 092–9
[28] Ghijsen J, Tjeng L H, van Elp J, Eskes H, Westerink J, Sawatzky G A and Czyzyk M T 1988 *Phys. Rev.* B **38** 11 322–30
[29] Chiba T 1976 *J. Chem. Phys.* **64** 1182–8
[30] Carel C, Mouallem-Bahout M and Gaude J 1999 *Solid State Ion.* **117** 47–55
[31] Galakhov V R, Finkelstein L D, Zatsepin D A, Kurmaev E Z, Samokhvalov A A, Naumov S V, Tatarinova G K, Demeter M, Bartkowski S, Neumann M and Moewes A 2000 *Phys. Rev.* B **62** 4922–6
[32] Wang S J, Wang B, Zhu J, Wang Z, Dai Y Q and He C Q 2001 *Mater. Sci. Forum* **363–365** 219–26
[33] Hermes H, Forster M and Schaefer H-E 1991 *Phys. Rev.* B **43** 10 399–403
[34] Alatalo M, Asoka-Kumar P, Ghosh V J, Nielsen B, Lynn K G, Kruseman A C, Van Veen A, Korhonen T and Puska M J 1998 *J. Phys. Chem. Solids* **59** 55–9
[35] Gizhevsky B A, Kozlov E A, Degtyarev M V, Voronova L M, Naumov S V and Tatarinova G N 1999 *Fiz. Khim. Obrab. Mater.* **3** 52–9 (in Russian)
[36] Samokhvalov A A, Viglin N A, Gizhevskii B A, Loshkareva N N, Osipov V V, Solin N I and Sukhorukov Yu P 1993 *Zh. Eksp. Teor. Fiz.* **103** 951–61 (Engl. transl. 1993 *Sov. Phys.–JETP* **76** 463–8)
[37] Gizhevskii B A, Galakhov V R, Zatsepin D A, Elokhina L V, Belykh T A, Kozlov E A, Naumov S V, Arbuzov V L, Shalnov K V and Neumann M 2002 *Fiz. Tverd. Tela* **44** 1318–25 (Engl. transl. 2002 *Sov. Phys.–Solid State* **44** 1380–7)